
STRUCTURAL SCIENCE
CRYSTAL ENGINEERING
MATERIALS

**Volume 75 (2019)**

**Supporting information for article:**

# Comparison of different strategies for modelling hydrogen atoms in charge density analyses

**Christian Köhler, Jens Lübben, Lennard Krause, Christina Hoffmann, Regine Herbst-Irmer and Dietmar Stalke**

**Table of Contents**

## S1. **Details about Application of Different H-Atom Approaches**

### S1.1. Neutron Data

As the H-ADPs derived from neutron data was used as reference for all approximation methods, special care was taken in the refinement against the neutron data set. Errors in the neutron refinement can easily result in faulty figures of merit, which can lead to wrong conclusions for the quality of approximate H-ADPs. For SPAnPS, two neutron data sets were available. In one dataset, all reflections with a significance lower than $3\sigma$ were omitted, the other dataset was not modified. Refinement against the unmodified data resulted in numerous cigar-shaped H-ADPs. As this is not chemically sound, the model obtained from the modified dataset was used for generating the reference H-ADPs. Data quality indicators of all neutron datasets can be found in Tables S1-S3. A refinement of all atomic positions and ADPs against the available neutron data was performed. The obtained H-ADPs were scaled to be compatible with X-ray data using *APD-Toolkit*. H-APDs and hydrogen-carbon distances were kept fixed for the refinement.

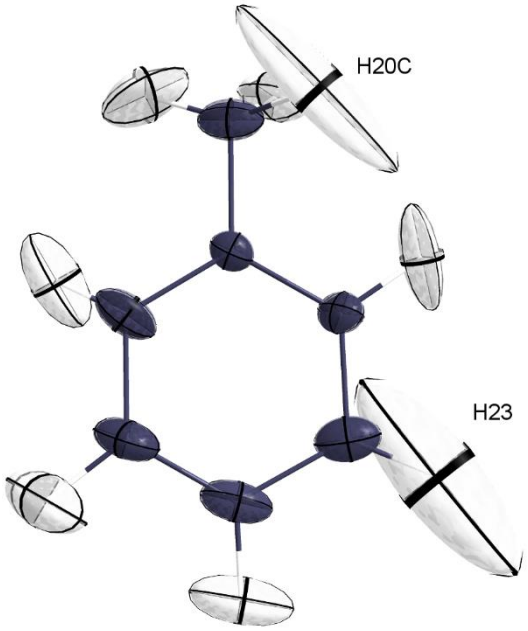


**Figure S1** Cigar-shaped hydrogen ADPs from the refinement against the unmodified neutron data. ADPs are displayed at 50 %probability level.

**Table S1** Data quality indicators including $R_{r.i.m.}$ and $R_{p.i.m.}$ (Weiss, 2001; Weiss & Hilgenfeld, 1997) given by *XPREP* (Sheldrick, 2014) for the unmodified neutron data of SPAnPS.

| *d [Å]* | *#Data* | *#hkl (theory)* | *%Comp* | *Redundancy* | $R_{r.i.m.}$ | $R_{p.i.m.}$ |
|---|---|---|---|---|---|---|
| Inf - 2.19 | 194 | 228 | 85.1 | 2.48 | 0.0772 | 0.0429 |
| 2.19 - 1.50 | 454 | 461 | 98.5 | 4.79 | 0.0882 | 0.0380 |
| 1.50 - 1.19 | 656 | 680 | 96.5 | 4.93 | 0.0634 | 0.0265 |
| 1.19 - 1.03 | 676 | 734 | 92.1 | 4.50 | 0.0687 | 0.0284 |
| 1.03 - 0.93 | 641 | 727 | 88.2 | 3.92 | 0.0817 | 0.0357 |
| 0.93 - 0.86 | 602 | 743 | 81.0 | 3.34 | 0.0997 | 0.0442 |
| 0.86 - 0.80 | 678 | 836 | 81.1 | 3.36 | 0.1013 | 0.0445 |
| 0.80 - 0.75 | 733 | 936 | 78.3 | 3.16 | 0.1116 | 0.0509 |
| 0.75 - 0.72 | 534 | 683 | 78.2 | 3.09 | 0.1169 | 0.0526 |
| 0.72 - 0.68 | 796 | 1110 | 71.7 | 2.68 | 0.1244 | 0.0573 |
| 0.68 - 0.65 | 714 | 1030 | 69.3 | 2.38 | 0.1507 | 0.0706 |
| 0.65 - 0.63 | 527 | 791 | 66.6 | 2.28 | 0.1424 | 0.0675 |
| 0.63 - 0.61 | 566 | 889 | 63.7 | 2.03 | 0.1550 | 0.0745 |
| 0.61 - 0.59 | 626 | 1036 | 60.4 | 1.90 | 0.1627 | 0.0783 |
| 0.59 - 0.57 | 696 | 1153 | 60.4 | 1.83 | 0.1521 | 0.0730 |
| 0.57 - 0.55 | 714 | 1366 | 52.3 | 1.36 | 0.1725 | 0.0873 |
| 0.55 - 0.53 | 647 | 1566 | 41.3 | 1.02 | 0.1861 | 0.0950 |
| 0.53 - 0.51 | 617 | 1804 | 34.2 | 0.68 | 0.2039 | 0.1155 |
| 0.51 - 0.49 | 557 | 2122 | 26.2 | 0.49 | 0.2002 | 0.1139 |
| 0.49 - 0.46 | 681 | 3933 | 17.3 | 0.29 | 0.2059 | 0.1208 |
| 0.46 - 0.40 | 591 | 11760 | 5.0 | 0.07 | 0.1913 | 0.1144 |

**Table S2** Data quality indicators given by *XPREP* for the neutron data of SPAnPS after rejection of reflections with a significance lower than 3 $\sigma$.

| *d [Å]* | *#Data* | *#hkl (theory)* | *%Comp* | *Redundancy* | $R_{r.i.m.}$ | $R_{p.i.m.}$ |
|---|---|---|---|---|---|---|
| Inf - 2.01 | 174 | 228 | 58.4 | 1.63 | 0.0353 | 0.0178 |
| 2.01 - 1.45 | 414 | 461 | 86.8 | 3.95 | 0.0455 | 0.0194 |
| 1.45 - 1.18 | 565 | 680 | 89.0 | 4.22 | 0.0409 | 0.0177 |
| 1.18 - 1.03 | 600 | 734 | 86.6 | 4.13 | 0.0440 | 0.0190 |
| 1.03 - 0.93 | 599 | 727 | 82.4 | 3.64 | 0.0596 | 0.0265 |
| 0.93 - 0.86 | 558 | 743 | 75.1 | 3.14 | 0.0747 | 0.0333 |
| 0.86 - 0.80 | 631 | 836 | 75.5 | 3.18 | 0.0799 | 0.0354 |
| 0.80 - 0.76 | 539 | 936 | 73.6 | 3.05 | 0.0924 | 0.0420 |
| 0.76 - 0.72 | 647 | 683 | 72.9 | 2.94 | 0.0974 | 0.0446 |
| 0.72 - 0.69 | 534 | 1110 | 65.9 | 2.53 | 0.1059 | 0.0492 |
| 0.69 - 0.66 | 632 | 1030 | 65.6 | 2.35 | 0.1205 | 0.0578 |
| 0.66 - 0.64 | 455 | 791 | 61.5 | 2.20 | 0.1247 | 0.0588 |
| 0.64 - 0.61 | 763 | 889 | 58.4 | 2.00 | 0.1352 | 0.0647 |
| 0.61 - 0.59 | 567 | 1036 | 54.7 | 1.78 | 0.1432 | 0.0687 |
| 0.59 - 0.57 | 627 | 1153 | 54.4 | 1.73 | 0.1381 | 0.0671 |
| 0.57 - 0.55 | 609 | 1366 | 44.6 | 1.25 | 0.1546 | 0.0783 |
| 0.55 - 0.53 | 567 | 1566 | 36.2 | 0.94 | 0.1680 | 0.0871 |
| 0.53 - 0.51 | 515 | 1804 | 28.5 | 0.61 | 0.1883 | 0.1051 |
| 0.51 - 0.49 | 462 | 2122 | 21.8 | 0.44 | 0.1951 | 0.1103 |
| 0.49 - 0.46 | 586 | 3933 | 14.9 | 0.27 | 0.2023 | 0.1186 |
| 0.46 - 0.40 | 483 | 11760 | 4.1 | 0.06 | 0.1864 | 0.1110 |

**Table S3** Data quality indicators given by *XPREP* for available the neutron data of SPAnH.

| *d [Å]* | *#Data* | *#hkl (theory)* | *%Comp* | *Redundancy* | $R_{r.i.m.}$ | $R_{p.i.m.}$ |
|---|---|---|---|---|---|---|
| Inf - 2.04 | 401 | 486 | 82.5 | 2.62 | 0.0805 | 0.0411 |
| 2.04 - 1.42 | 925 | 960 | 96.4 | 4.46 | 0.0754 | 0.0329 |
| 1.42 - 1.13 | 1333 | 1403 | 95.0 | 4.35 | 0.0818 | 0.0350 |
| 1.13 - 0.99 | 1315 | 1426 | 92.2 | 4.03 | 0.1006 | 0.0431 |
| 0.99 - 0.89 | 1463 | 1601 | 91.4 | 3.66 | 0.1441 | 0.0642 |
| 0.89 - 0.83 | 1212 | 1359 | 89.2 | 3.46 | 0.1594 | 0.0710 |
| 0.83 - 0.78 | 1303 | 1476 | 88.3 | 3.35 | 0.1617 | 0.0740 |
| 0.78 - 0.74 | 1333 | 1498 | 89.0 | 3.27 | 0.1727 | 0.0791 |
| 0.74 - 0.70 | 1607 | 1863 | 86.3 | 3.04 | 0.1758 | 0.0813 |
| 0.70 - 0.67 | 1394 | 1685 | 82.7 | 2.65 | 0.1977 | 0.0954 |
| 0.67 - 0.65 | 1101 | 1307 | 84.2 | 2.64 | 0.2142 | 0.1033 |
| 0.65 - 0.63 | 1236 | 1493 | 82.8 | 2.54 | 0.2155 | 0.1044 |
| 0.63 - 0.61 | 1354 | 1678 | 80.7 | 2.39 | 0.2282 | 0.1113 |
| 0.61 - 0.59 | 1542 | 1905 | 80.9 | 2.34 | 0.2292 | 0.1125 |
| 0.59 - 0.57 | 1707 | 2205 | 77.4 | 2.09 | 0.2421 | 0.1223 |
| 0.57 - 0.56 | 898 | 1199 | 74.9 | 1.94 | 0.2496 | 0.1283 |
| 0.56 - 0.54 | 1985 | 2728 | 72.8 | 1.73 | 0.2738 | 0.1446 |
| 0.54 - 0.53 | 1050 | 1506 | 69.7 | 1.49 | 0.2835 | 0.1560 |
| 0.53 - 0.52 | 1090 | 1631 | 66.8 | 1.40 | 0.2932 | 0.1628 |
| 0.52 - 0.51 | 1103 | 1741 | 63.4 | 1.21 | 0.3000 | 0.1706 |
| 0.51 - 0.50 | 1108 | 1946 | 56.9 | 1.04 | 0.3337 | 0.1981 |

### S1.2. *SHADE* 2.1

All necessary information for the *SHADE* procedure was obtained from a crystallographic information file (.cif) generated with *XDCIF* in the *XD2016* program suite (Volkov *et al.*, 2016) from the refinement against X-ray data. The parameter file from the final refinement step was update with H-ADPs assigned by the *SHADE2.1* server and then submitted to a refinement of the scale factors in a first step and refinement of all previously refined variables except $\kappa'$ and H-ADPs, which were kept fixed on the obtained anisotropic *SHADE* values.

### *S1.3. APD-Toolkit*

The XD parameter file of the final isotropic hydrogen refinement was loaded into *APD-Toolkit*. An automated segmented rigid body TLS was performed. All H-ADPs written in the output XD parameter file were copied into the first input parameter file of the isotropic refinement strategy. The refinement progress was repeated with the new parameter file. All H-ADPs were kept fixed on the obtained anisotropic *APD-Toolkit* values.

### S1.4. Free Anisotropic Refinement

A last final step was added to the refinement, in which all constraints for isotropic H-atoms were released. All hydrogen displacement parameters were refined in addition to all previously refined parameters.

## S2. Additional Information for SPAnPS

### S2.1. Data Collection

The high-resolution data for SPAnPS, was collected in 2007 at $T = 100$ K on a Bruker D8 three-circle goniometer equipped with a Smart APEX II CCD, a TXS Mo rotating anode, Incoatec Helios mirror optics and a Bruker Kryoflex II device. Data was collected in 21 runs. In runs 1-13, low order data up to $d = 0.7$ Å were collected. In runs 14-21, high order data up to $d = 0.44$ Å was collected. During the evaluation of the collected data, areas with to high recorded intensities were found on several frames. Masking the contaminated areas was attempted, but lead to worsening of data quality indicators. For the final data integration, all contaminated frames were omitted (Figures S2, S3).

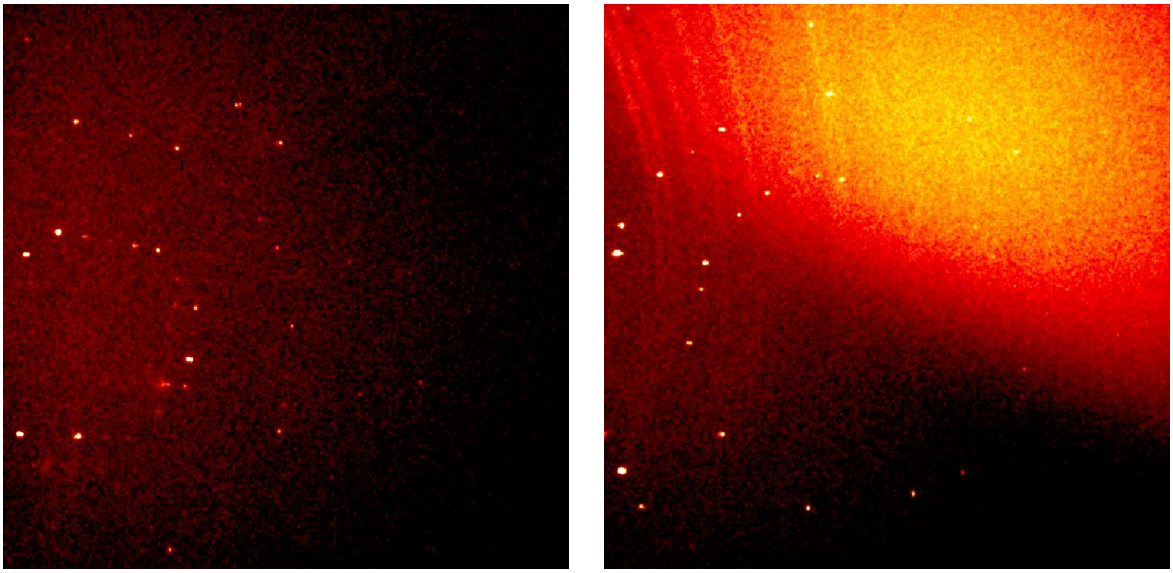

**Figure S2** : Left: Uncontaminated frame ($\omega = 285°$) from run 14. Right: Contaminated frame from the same run ($\omega = 265.5°$). The overexposed area in the top right part of the frame is clearly visible. Observations were similar for runs 14, 15, 18, 19, 20, 21. Contaminated frames were omitted for the final integration.

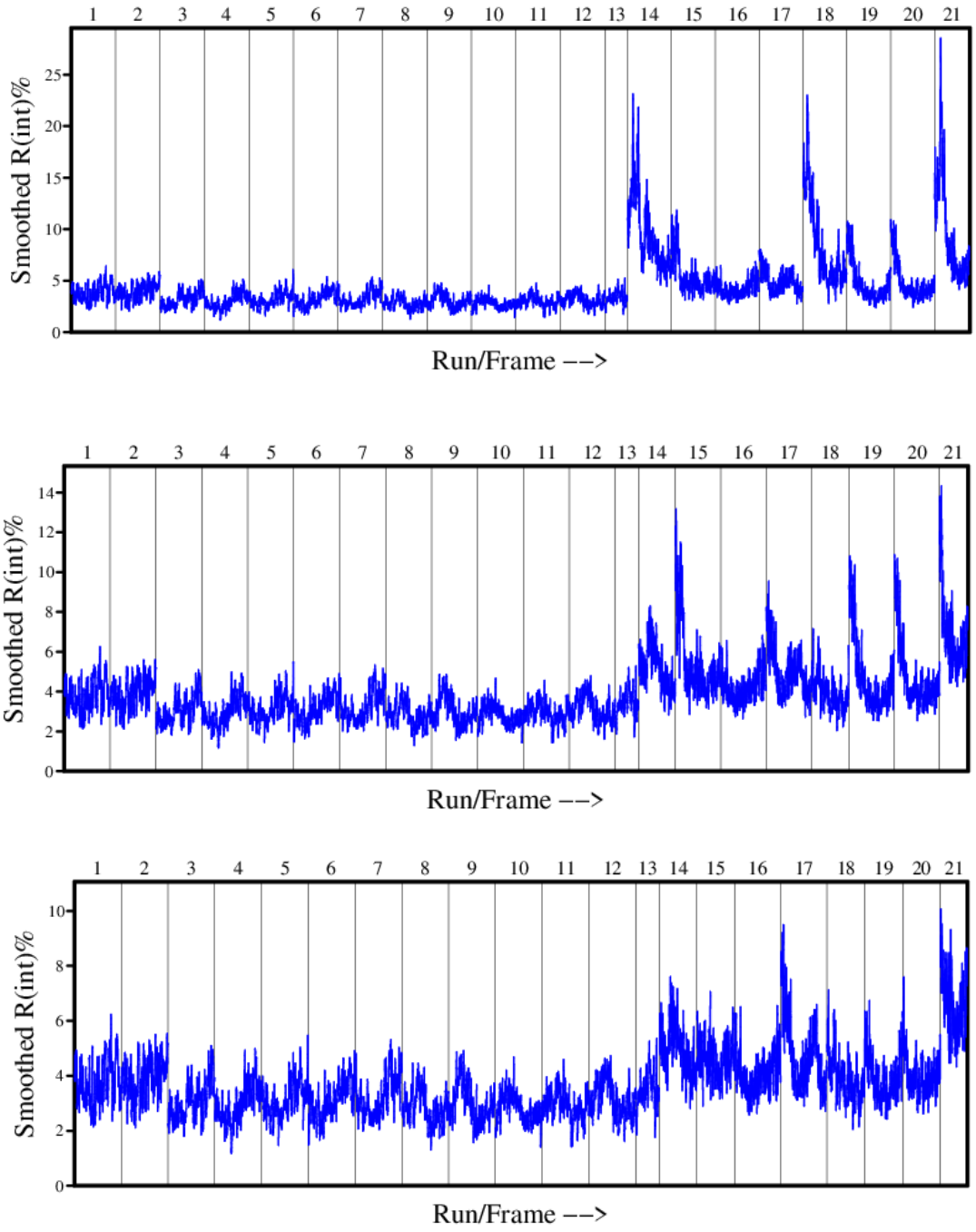


**Figure S3** Effects of stepwise removal of problematic frames on the $R_{int}$ plot generated by *SADABS* (Krause *et al.*, 2015). Top: All frames are integrated. Middle: The first 109 frames of runs 14, 18 and 21 were omitted from integration ($265.3° \leq \omega \leq 285.0$). Bottom: Additionally, the first 109 frames of runs 15, 19 and 20 were removed. Twenty additional frames were removed from run 21 (up to $\omega \leq$ 246.3°).

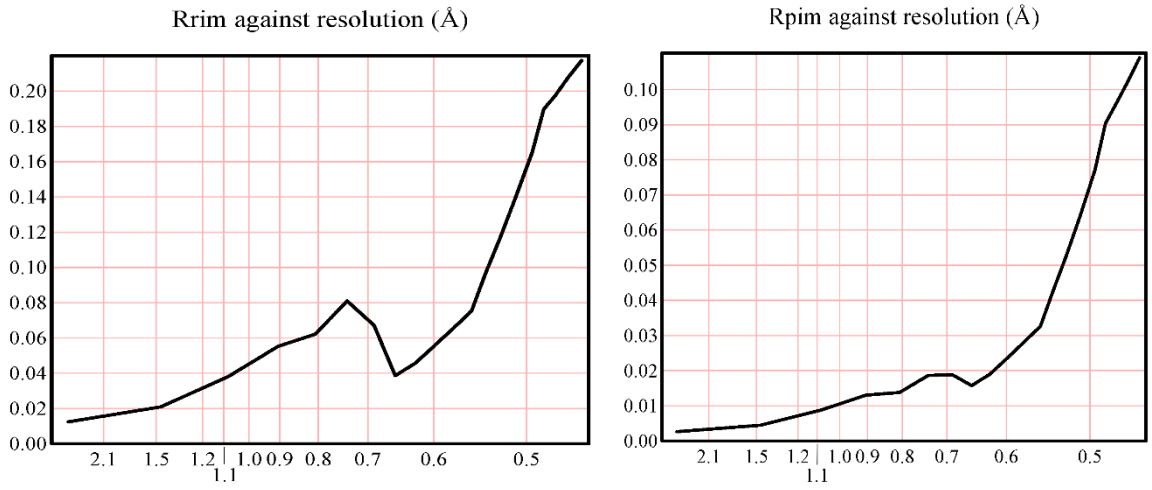


**Figure S4** Course of $R_{r.i.m.}$ and $R_{p.i.m.}$ with resolution for SPAnPS.

**Table S4** Data quality indicators given by *XPREP*. For the final integration, a resolution cut-off at $d = 0.45$ was performed due to a strong increase of both $R_{r.i.m.}$ and $R_{p.i.m.}$ and a strong decrease of the completeness at higher resolution.

| *d [Å]* | *#Data* | *#hkl (theory)* | *%Comp* | *Redundancy* | $R_{r.i.m.}$ | $R_{p.i.m.}$ |
|---|---|---|---|---|---|---|
| Inf - 1.83 | 392 | 392 | 100 | 21.15 | 0.0126 | 0.0027 |
| 1.83 - 1.21 | 914 | 914 | 100 | 21.75 | 0.0211 | 0.0045 |
| 1.21 - 0.95 | 1358 | 1358 | 100 | 18.21 | 0.0407 | 0.0095 |
| 0.95 - 0.83 | 1294 | 1294 | 100 | 18.53 | 0.0551 | 0.0128 |
| 0.83 - 0.75 | 1406 | 1406 | 100 | 19.82 | 0.0671 | 0.015 |
| 0.75 - 0.7 | 1216 | 1216 | 100 | 18.2 | 0.087 | 0.0202 |
| 0.7 - 0.66 | 1252 | 1252 | 100 | 6.02 | 0.0358 | 0.0145 |
| 0.66 - 0.62 | 1597 | 1597 | 100 | 5.8 | 0.0423 | 0.0174 |
| 0.62 - 0.6 | 959 | 959 | 100 | 5.61 | 0.0524 | 0.022 |
| 0.6 - 0.57 | 1699 | 1699 | 100 | 5.39 | 0.0605 | 0.0258 |
| 0.57 - 0.55 | 1366 | 1366 | 100 | 5.12 | 0.0748 | 0.0324 |
| 0.55 - 0.53 | 1574 | 1574 | 100 | 4.99 | 0.097 | 0.0428 |
| 0.53 - 0.52 | 865 | 865 | 100 | 4.77 | 0.1171 | 0.0528 |
| 0.52 - 0.5 | 1955 | 1955 | 100 | 4.62 | 0.1402 | 0.0642 |
| 0.5 - 0.49 | 1114 | 1114 | 100 | 4.49 | 0.1656 | 0.0773 |
| 0.49 - 0.48 | 1193 | 1193 | 100 | 4.29 | 0.1903 | 0.0907 |
| 0.48 - 0.47 | 1309 | 1309 | 100 | 4.14 | 0.1981 | 0.0962 |
| 0.47 - 0.46 | 1439 | 1439 | 100 | 3.98 | 0.2082 | 0.1024 |
| 0.46 - 0.45 | 1517 | 1517 | 100 | 3.8 | 0.2167 | 0.1081 |
| 0.45 - 0.44 | 1559 | 1696 | 91.92 | 2.8 | 0.2426 | 0.1306 |

**DRK-Plots**

**S2.1.1. One Scale Factor**

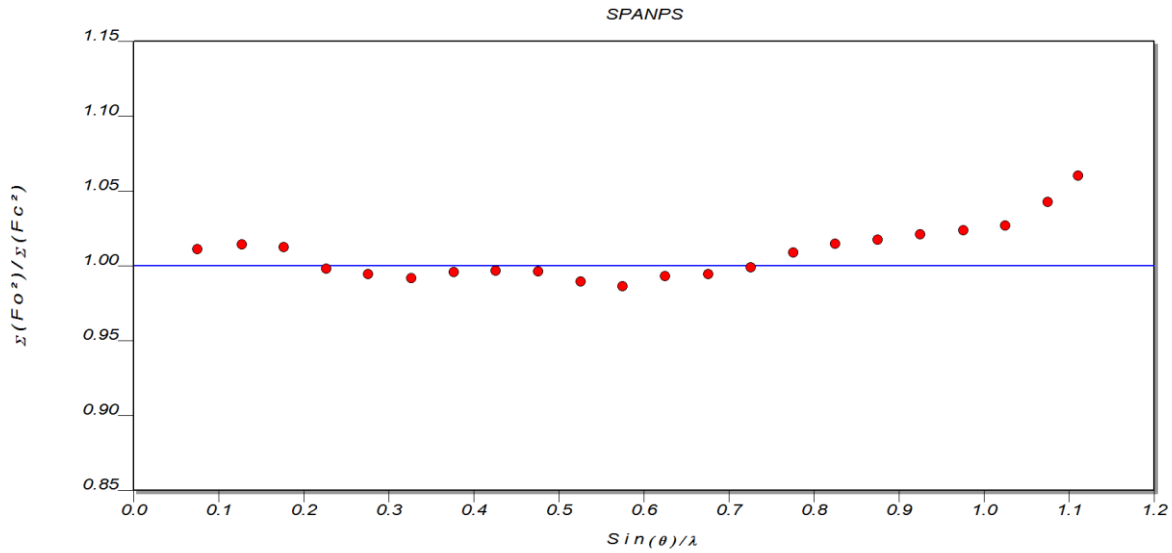


**Figure S5** Plot of $\Sigma F_o^2 / \Sigma F_c^2$ against the resolution for the initial refinement of SPAnPS. A deviation from unity larger than 5 % is indicative of errors in the data (Adam Stash, 2007).

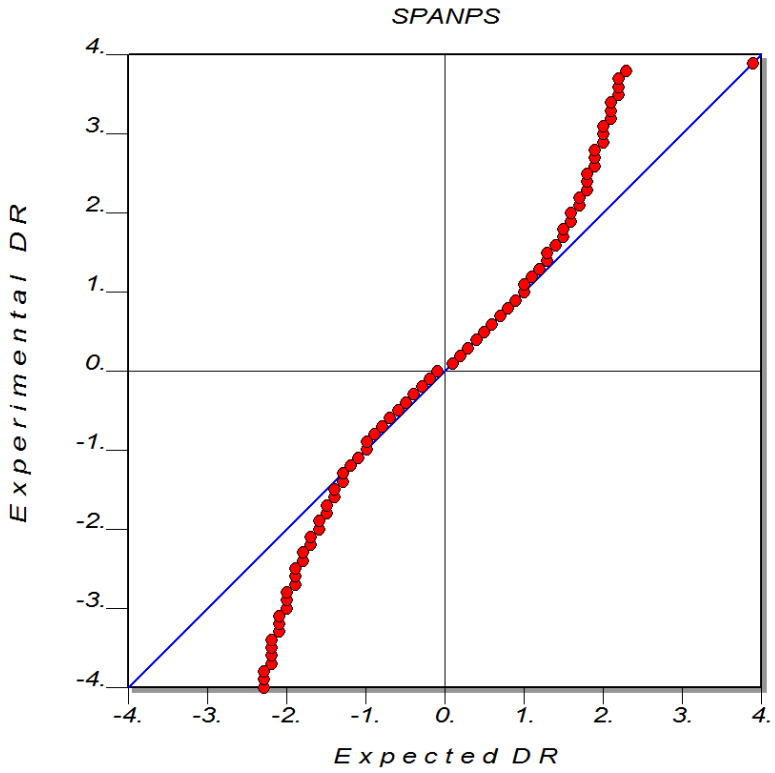


**Figure S6** Normal probability plot for the refinement with one scale factor (Adam Stash, 2007).

### S2.1.2. 10 Scale Factors

The shape of the plot shown in Figure S5 shows resolution dependent errors, but has not the characteristic shape of caused by thermal diffuse scattering (TDS) (Willis, 2001). Therefore, the final refinement was conducted with 10 resolution-dependent scale factors.

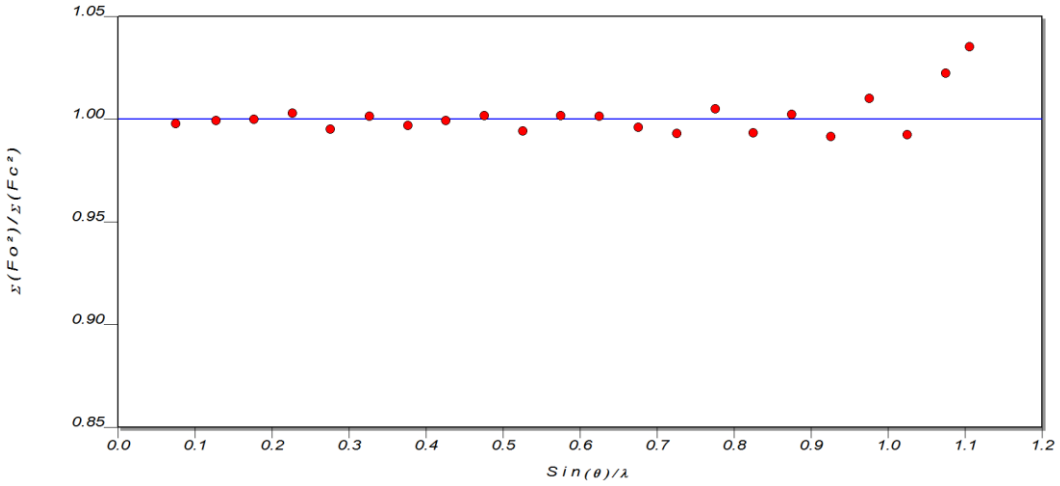


**Figure S7** Plot of $\Sigma F_o^2/\Sigma F_c^2$ against resolution for refinement with ten resolution-dependent scale factors after application of H-ADPs derived from neutron data. Even for high-order reflections, a value of 1.05 is not exceeded anymore.

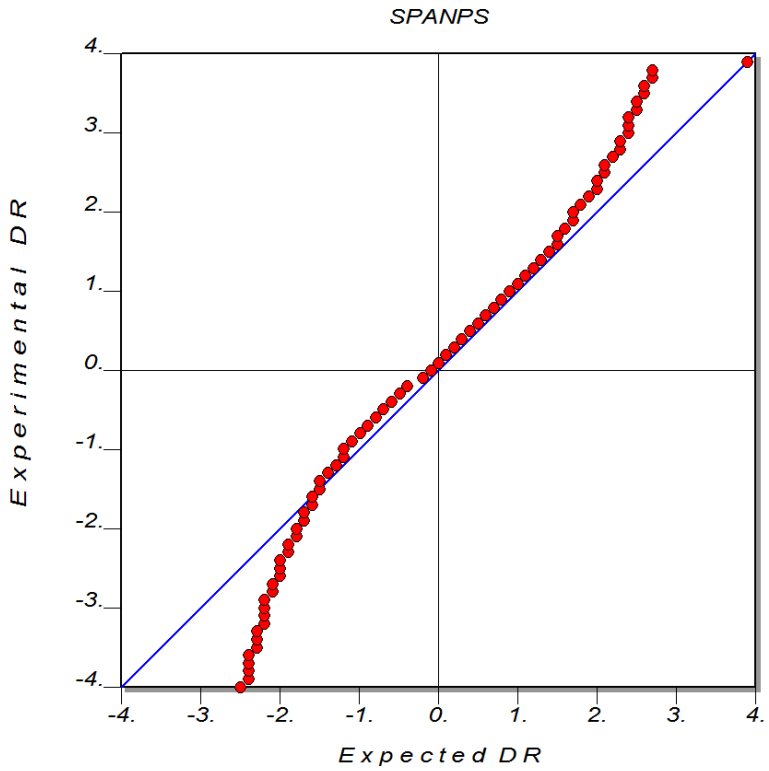


**Figure S8** Normal probability plot for the refinement with 10 scale factors.

### S2.2. Local Coordinate Systems

| ATOM | ATOM0 | AX1 | ATOM1 | ATOM2 | AX2 | R/L | TP | TBL | KAP | LMX | SITESYM | CHEMCON |
|---|---|---|---|---|---|---|---|---|---|---|---|---|
| S1 | P1 | Z | S1 | C2 | Y | R | 4 | 1 | 1 | 4 | _6 | |
| P1 | S1 | Z | P1 | C14 | Y | R | 4 | 2 | 2 | 4 | _6 | |
| C1 | C2 | X | C1 | C3 | Y | R | 2 | 3 | 3 | 4 | _mz | |
| C2 | P1 | Z | C2 | C3 | X | R | 2 | 3 | 4 | 4 | _mm2 | |
| C3 | C2 | X | C3 | C4 | Y | R | 2 | 3 | 3 | 4 | _mz | C1 |
| C4 | C3 | X | C4 | C5 | Y | R | 2 | 3 | 5 | 4 | _mz | |
| C5 | C4 | X | C5 | C6 | Y | R | 3 | 3 | 6 | 4 | _mz | |
| C6 | C5 | X | C6 | C7 | Y | R | 3 | 3 | 6 | 4 | _mz | C5 |
| C7 | C6 | X | C7 | C5 | Y | R | 2 | 3 | 5 | 4 | _mm2 | C4 |
| C8 | P1 | Z | C8 | C13 | Y | R | 2 | 3 | 7 | 4 | _mz | |
| C9 | C8 | X | C9 | C10 | Y | R | 3 | 3 | 8 | 4 | _mz | |
| C10 | DUM0 | Z | C10 | C11 | X | R | 3 | 3 | 9 | 4 | _mm2 | |
| C11 | DUM1 | Z | C11 | C12 | X | R | 3 | 3 | 9 | 4 | _mm2 | C10 |
| C12 | DUM2 | Z | C12 | C13 | X | R | 3 | 3 | 9 | 4 | _mm2 | C10 |
| C13 | C8 | X | C13 | C12 | Y | R | 2 | 3 | 8 | 4 | _mz | C9 |
| C14 | P1 | Z | C14 | C19 | Y | R | 2 | 3 | 7 | 4 | _mm2 | C8 |
| C15 | C14 | X | C15 | C16 | Y | R | 2 | 3 | 8 | 4 | _mz | C9 |
| C16 | DUM3 | Z | C16 | C17 | X | R | 3 | 3 | 9 | 4 | _mm2 | C10 |
| C17 | DUM4 | Z | C17 | C18 | X | R | 3 | 3 | 9 | 4 | _mm2 | C10 |
| C18 | DUM5 | Z | C18 | C19 | X | R | 3 | 3 | 9 | 4 | _mm2 | C10 |
| C19 | C14 | X | C19 | C18 | Y | R | 2 | 3 | 8 | 4 | _mz | C9 |
| C20 | C21 | Z | C20 | H20C | X | R | 3 | 4 | 10 | 4 | _3my | |
| C21 | C20 | X | C21 | C26 | Y | R | 3 | 3 | 11 | 4 | _mz | |
| C22 | C21 | X | C22 | C23 | Y | R | 3 | 3 | 12 | 4 | _mz | |

| | | | | | | | | | | | | |
|---|---|---|---|---|---|---|---|---|---|---|---|---|
| C23 | DUM6 | Z | C23 | C24 | X | R | 3 | 3 | 13 | 4 | _mm2 | |
| C24 | DUM7 | Z | C24 | C25 | X | R | 3 | 3 | 13 | 4 | _mm2 | C23 |
| C25 | DUM8 | Z | C25 | C26 | X | R | 3 | 3 | 13 | 4 | _mm2 | C23 |
| C26 | C21 | X | C26 | C25 | Y | R | 3 | 3 | 12 | 4 | _mz | C22 |
| H4 | C4 | Z | H4 | C3 | Y | R | 2 | 5 | 14 | 2 | _6 | |
| H5 | C5 | Z | H5 | C4 | Y | R | 2 | 5 | 14 | 2 | _6 | H4 |
| H6 | C6 | Z | H6 | C5 | Y | R | 2 | 5 | 14 | 2 | _6 | H4 |
| H7 | C7 | Z | H7 | C6 | Y | R | 2 | 5 | 14 | 2 | _6 | H4 |
| H9 | C9 | Z | H9 | C8 | Y | R | 2 | 5 | 14 | 2 | _6 | H4 |
| H10 | C10 | Z | H10 | C9 | Y | R | 2 | 5 | 14 | 2 | _6 | H4 |
| H11 | C11 | Z | H11 | C10 | Y | R | 2 | 5 | 14 | 2 | _6 | H4 |
| H12 | C12 | Z | H12 | C11 | Y | R | 2 | 5 | 14 | 2 | _6 | H4 |
| H13 | C13 | Z | H13 | C8 | Y | R | 2 | 5 | 14 | 2 | _6 | H4 |
| H15 | C15 | Z | H15 | C14 | Y | R | 2 | 5 | 14 | 2 | _6 | H4 |
| H16 | C16 | Z | H16 | C15 | Y | R | 2 | 5 | 14 | 2 | _6 | H4 |
| H17 | C17 | Z | H17 | C16 | Y | R | 2 | 5 | 14 | 2 | _6 | H4 |
| H18 | C18 | Z | H18 | C17 | Y | R | 2 | 5 | 14 | 2 | _6 | H4 |
| H19 | C19 | Z | H19 | C14 | Y | R | 2 | 5 | 14 | 2 | _6 | H4 |
| H20A | C20 | Z | H20A | H20B | Y | R | 2 | 5 | 15 | 2 | _6 | |
| H20B | C20 | Z | H20B | H20A | Y | R | 2 | 5 | 15 | 2 | _6 | H20A |
| H20C | C20 | Z | H20C | H20A | Y | R | 2 | 5 | 15 | 2 | _6 | H20A |
| H22 | C22 | Z | H22 | C21 | Y | R | 2 | 5 | 14 | 2 | _6 | H4 |
| H23 | C23 | Z | H23 | C22 | Y | R | 2 | 5 | 14 | 2 | _6 | H4 |
| H24 | C24 | Z | H24 | C23 | Y | R | 2 | 5 | 14 | 2 | _6 | H4 |
| H25 | C25 | Z | H25 | C24 | Y | R | 2 | 5 | 14 | 2 | _6 | H4 |
| H26 | C26 | Z | H26 | C21 | Y | R | 2 | 5 | 14 | 2 | _6 | H4 |

**S2.3. Refinement Strategy**

**Table S5** Final refinement strategy for SPAnPS with isotropic hydrogen atoms. Starting values for multipole and $\kappa$- parameters were obtained from the *INVARIOM* database (Dittrich *et al.*, 2013) using the software *InvariomTool* (Luger *et al.*, 2007). The ten scale factors are refined in each step. Red denotes newly added parameters. Green denotes the final refinement step with fixed C-H bond distances. At the beginning of the refinement, only reflections with a significance of at least 3$\sigma$ are taken into account ("sigobs 3"). This limitation is released in step 10. A test for overfitting was performed using a $R_{cross}$ as validation tool.(Krause *et al.*, 2017b). Abbreviations: M: monopoles; D: dipoles; Q: quadrupoles; O: octupoles; H: hexadecapoles, U: Uij, k: kappa, U3/4 (atom name): Gram Charlier 3$^{rd}$/4$^{th}$ order, nosym: no local symmetry constraints, nocon: no chemical constraints, *d/p*: data to parameter ratio, $d_1/p_m$: ratio of low resolution data ( up to 1 Å) to multipole parameter.

**Table S6**

| Step | Parameters | #param | #data | $d/p$ | $d_1/p_m$ | $\sigma$ cut-off | $R(F^2)$ |
|---|---|---|---|---|---|---|---|
| 1 | SCALE | 10 | 16587 | 1658.7 | None | 3 | 0.0342 |
| 2 | U | 178 | 16587 | 93.19 | None | 3 | 0.0327 |
| 3 | Uxyz | 262 | 16587 | 63.31 | None | 3 | 0.0282 |
| 4 | MDQOHUxyz | 414 | 16587 | 40.07 | 25.06 | 3 | 0.022 |
| 5 | MDQOHUxyz$\kappa$ | 427 | 16587 | 38.85 | 21.63 | 3 | 0.0211 |
| 6 | xyz(H) | 76 | 2146 | 28.24 | None | 3 | 0.0205 |
| 7 | MDQOHUxyz$\kappa$ | 427 | 16587 | 38.85 | 21.63 | 3 | 0.0205 |
| 8 | $\kappa'$ | 23 | 16587 | 721.17 | None | 3 | 0.0204 |
| 9 | MDQOHUxyz$\kappa$ | 427 | 16587 | 38.85 | 21.63 | 3 | 0.0202 |
| 10 | Sigobs 0 | 427 | 22130 | 51.83 | 22.59 | 0 | 0.0202 |
| 11 | MDQOHUxyz$\kappa$ U3 (S1, P1, C9-12, C20-21, C24-26) | 537 | 22130 | 41.21 | 22.59 | 0 | 0.0179 |
| 12 | MDQOHUxyz$\kappa$ U3 (C5-6, C22-23, C16-18) | 607 | 22130 | 36.46 | 22.59 | 0 | 0.0173 |
| 13 | MDQOHUxyz$\kappa$ U3 , U4 (S1, P1) | 622 | 22130 | 35.58 | 22.59 | 0 | 0.0172 |

| | | | | | | | |
|---|---|---|---|---|---|---|---|
| 14 | $\kappa'$ | 23 | 22130 | 962.17 | None | 0 | 0.0171 |
| 15 | MDQOHUxyz$\kappa$, U3, U4 | 637 | 22130 | 34.74 | 22.59 | 0 | 0.0169 |
| 16 | H-Uij unconstrained | 769 | 22130 | 28.78 | 22.59 | 0 | 0.0148 |
| 17 | Nocon Anthracene | 814 | 22130 | 27.19 | 18.5 | 0 | 0.0147 |
| 18 | H(xyz) without RESET | 880 | 22130 | 25.15 | 18.5 | 0 | 0.0142 |

**Release of Constraints**

| Step | Parameters | #param | #data | $d/p$ | $d_1/p_m$ | $\sigma$ cut-off | $R(F^2)$ |
|---|---|---|---|---|---|---|---|
| 1-18 | As before | | | | | | |
| 19 | Nosymm P | 111 | 2146 | 24.7 | 17.31 | 0 | 0.0142 |
| 20 | Nosymm S | 121 | 2146 | 24.16 | 16.01 | 0 | 0.0141 |
| 21 | Nosymm | 215 | 2146 | 20.17 | 9.41 | 0 | 0.0135 |
| 22 | Nocon | 439 | 2146 | 14.32 | 4.75 | 0 | 0.0122 |

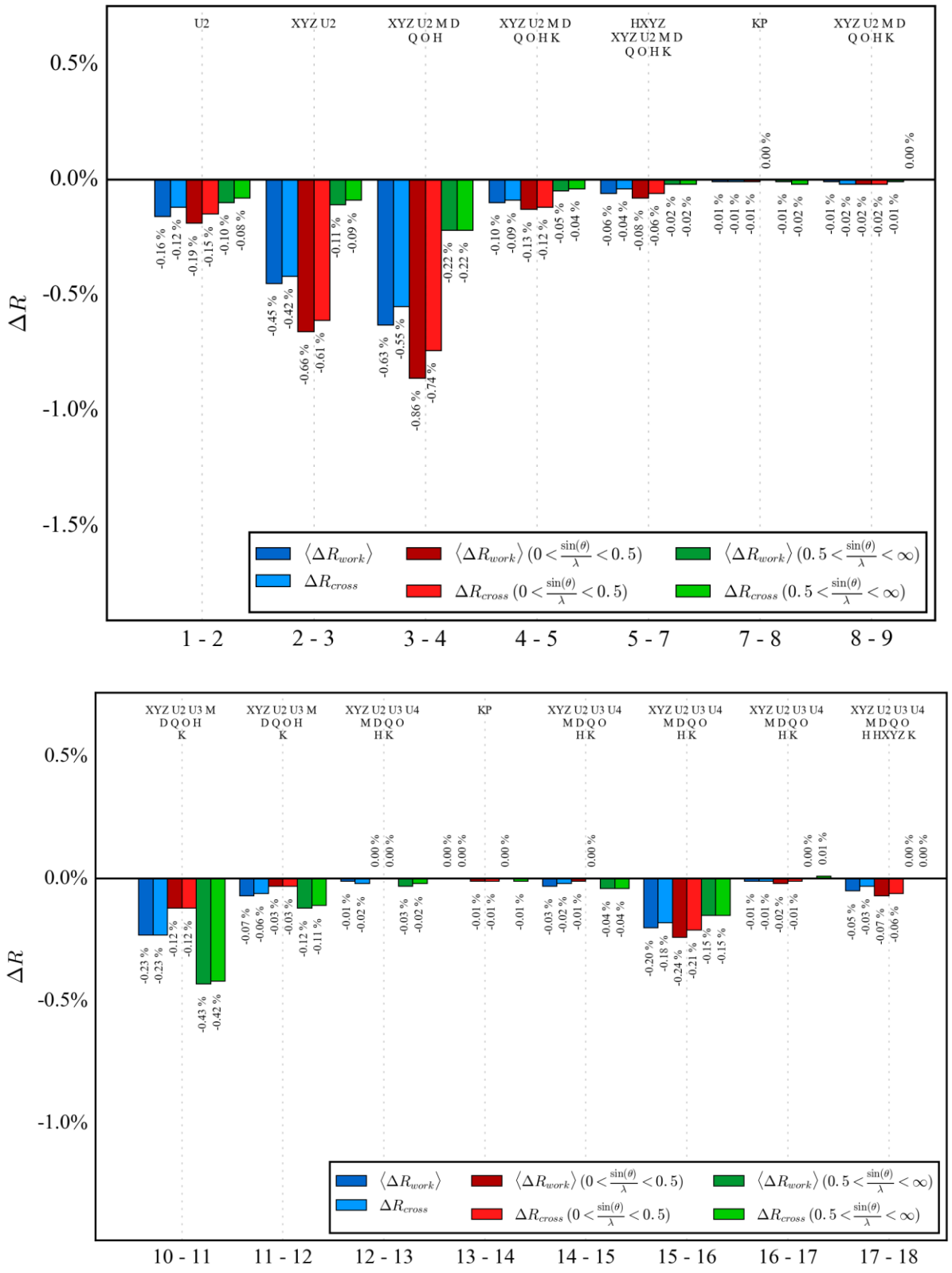


**Figure S9** Cross-validation output plot for steps included in the final refinement of SPAnPS. The generally joined improvement of both $R_{work}$ and $R_{cross}$ indicates that all introduced parameters are meaningful.

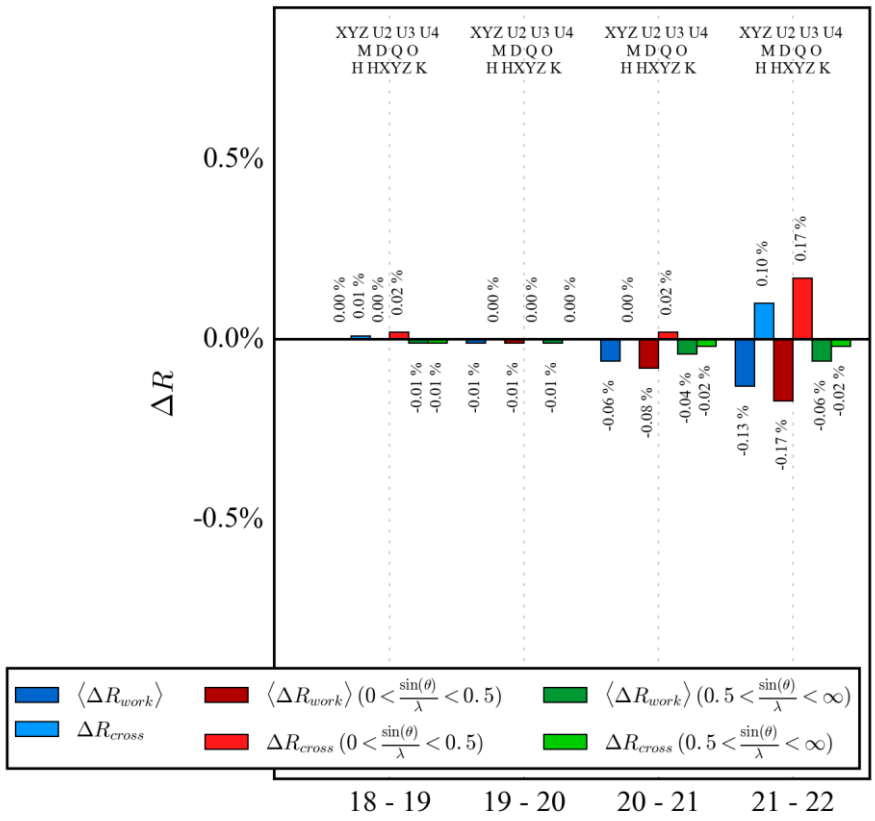


**Figure S10** Cross-validation output plot for steps excluded from the final refinement of SPAnPS. All steps include a worsening of the $R_{cross}$ while $R_{work}$ stays constant or improves. This is a sign of overfitting.

## S2.4. Residuals After Final Refinement Step against X-ray Data with Fixed C-H Distances

### S2.4.1. Neutron ADPs with Neutron Distances

| | | | | | | | | |
|---|---|---|---|---|---|---|---|---|
| $R(F)$ | = | 0.0258 | $R_{all}(F)$ | = | 0.0258 | $R_w(F)$ | = | 0.0095 |
| $R(F^2)$ | = | 0.0155 | $R_{all}(F^2)$ | = | 0.0155 | $R_w(F^2)$ | = | 0.0184 |
| GOF*w* | = | 1.2871 | GOF | = | 1.2871 | $N_{ref}/N_v$ | = | 32.4487 |

### S2.4.2. SHADE

| | | | | | | | | |
|---|---|---|---|---|---|---|---|---|
| $R(F)$ | = | 0.0266 | $R_{all}(F)$ | = | 0.0266 | $R_w(F)$ | = | 0.0101 |
| $R(F^2)$ | = | 0.0169 | $R_{all}(F^2)$ | = | 0.0169 | $R_w(F^2)$ | = | 0.0198 |
| GOF*w* | = | 1.3865 | GOF | = | 1.3865 | $N_{ref}/N_v$ | = | 32.4487 |

### S2.4.3. APD-Toolkit

| | | | | | | | | |
|---|---|---|---|---|---|---|---|---|
| $R(F)$ | = | 0.0261 | $R_{all}(F)$ | = | 0.0261 | $R_w(F)$ | = | 0.0097 |
| $R(F^2)$ | = | 0.0161 | $R_{all}(F^2)$ | = | 0.0161 | $R_w(F^2)$ | = | 0.0189 |
| GOF*w* | = | 1.3212 | GOF | = | 1.3212 | $N_{ref}/N_v$ | = | 32.4487 |

### S2.4.4. Aniso without H-Q0

| | | | | | | | | |
|---|---|---|---|---|---|---|---|---|
| $R(F)$ | = | 0.0254 | $R_{all}(F)$ | = | 0.0254 | $R_w(F)$ | = | 0.0090 |
| $R(F^2)$ | = | 0.0147 | $R_{all}(F^2)$ | = | 0.0147 | $R_w(F^2)$ | = | 0.0174 |
| GOF*w* | = | 1.2231 | GOF | = | 1.2231 | $N_{ref}/N_v$ | = | 27.2537 |

### S2.4.5. Aniso with H-Q0

| | | | | | | | | |
|---|---|---|---|---|---|---|---|---|
| $R(F)$ | = | 0.0254 | $R_{all}(F)$ | = | 0.0254 | $R_w(F)$ | = | 0.0090 |
| $R(F^2)$ | = | 0.0146 | $R_{all}(F^2)$ | = | 0.0146 | $R_w(F^2)$ | = | 0.0174 |
| GOF*w* | = | 1.2229 | GOF | = | 1.2229 | $N_{ref}/N_v$ | = | 27.1867 |

## S2.5. Refinement of Anharmonic Motion

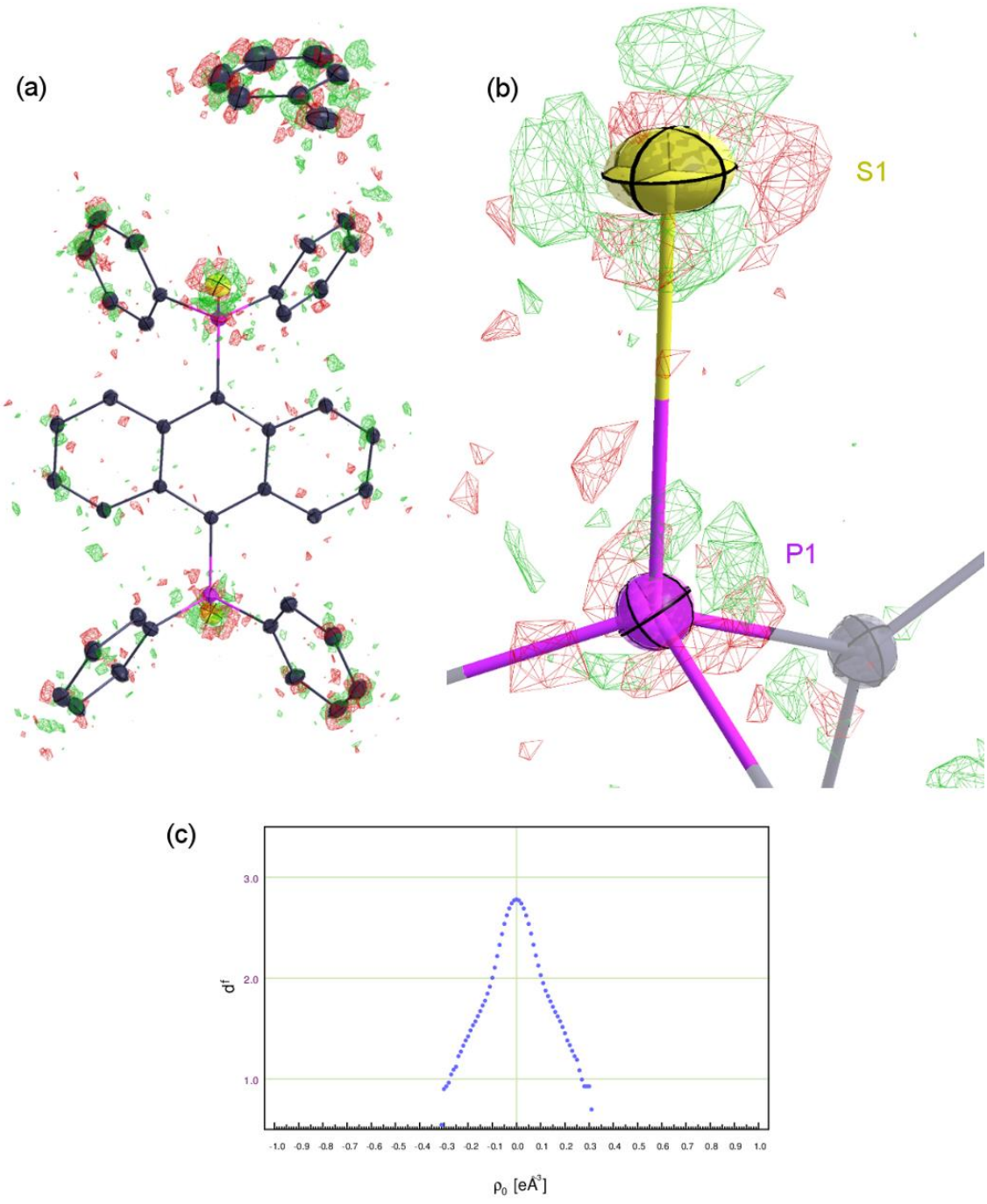


**Figure S11**(a): Residual density map of the asymmetric unit of SPAnPS before introduction of Gram-Charlier parameters (Johnson & Levy, 1974) in step 11. H-Atoms are omitted for visual clarity. Isolevel for residual density: $\pm$ 0.093Å$^{-3}$. ADPs are depicted at 50 % probability level. (b): Close-up on the shashlik-shaped residual density around S1 and P1. (c): Henn-Meindl plot of the residual density (Meindl & Henn, 2008). The broadening of the parabola is indicative for an excess of both positive and negative residual density.

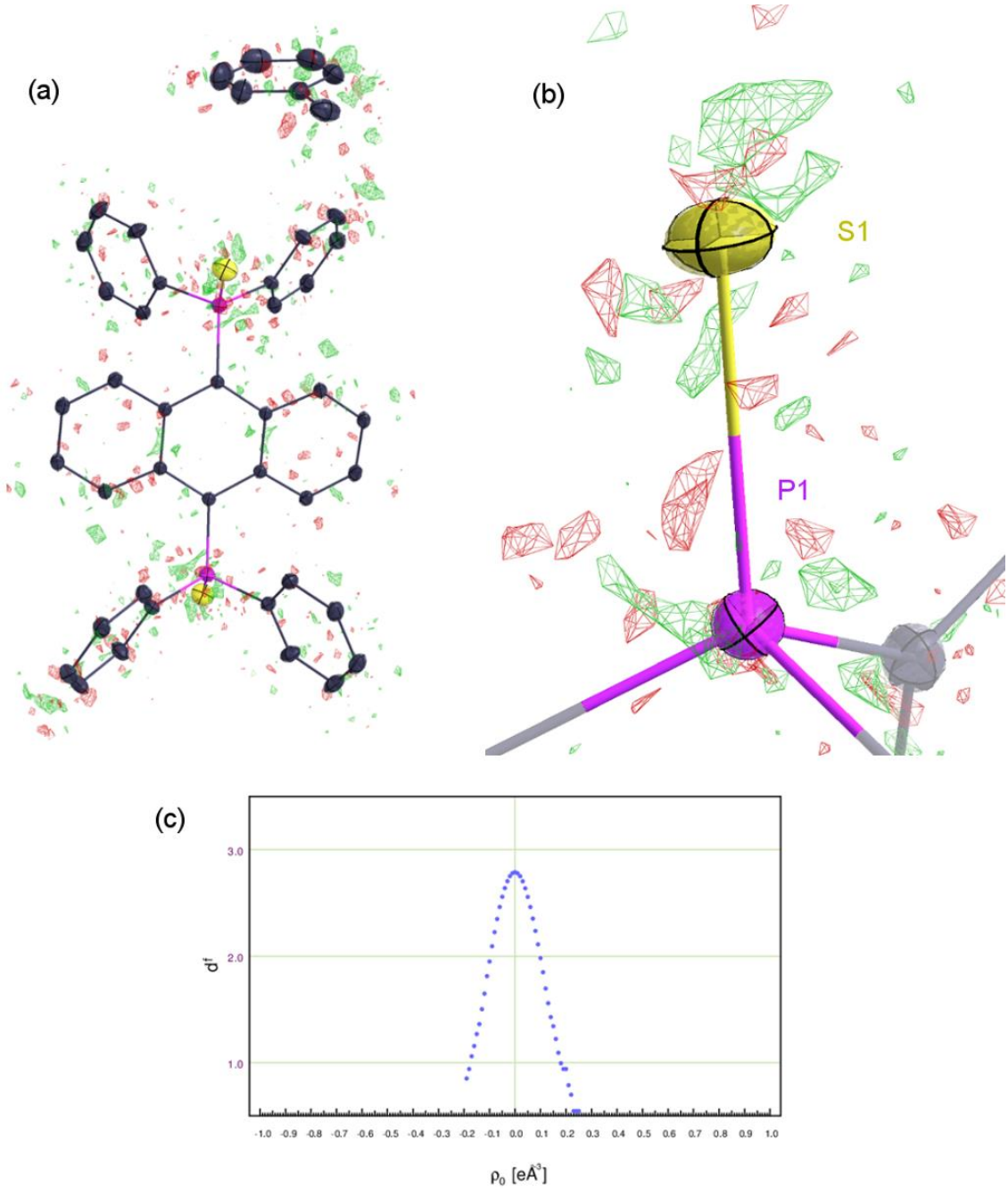


**Figure S12** (a): Residual density map of the asymmetric unit of SPAnPS after introduction of Gram-Charlier parameters. H-Atoms are omitted for visual clarity. Isolevel for residual density: $\pm$ 0.084Å$^{-3}$. (b): Close-up on greatly reduced residual density around S1 and P1. ADPs are depicted at 50 % probability level. (c): Improved Henn-Meindl plot of the residual density after introduction of Gram-Charlier coefficients.

**Table S7** Selected model quality indicators before and after the refinement of Gram-Charlier coefficients of 3rd and 4th order (Johnson & Levy, 1974).

| | $R$ [%] | $e_{\mathrm{gross}}$ [e] | $d^f(0)$ | highest peak [e · Å$^{-3}$] | deepest hole [e · Å$^{-3}$] |
|---|---|---|---|---|---|
| harmonic | 2.06 | 28.7 | 2.77 | 0.35 | 0.32 |
| anharmonic | 1.73 | 26.8 | 2.77 | 0.23 | 0.22 |

### S2.5.1. Closer Inspection of Probability Density Functions

**Table S8** Data regarding the significance of the probability density functions (pdfs) for atomic displacement resulting from refined Gram-Charlier coefficient and negative regions of the resulting atomic displacements pdfs. 4th order coefficients were only refined for S1 and P1, all other refined GCCs are of 3rd order.

| | *Significance of most sign. GCC* [$GCC/esd$] | *Minimum of pdf* | *Integrated negative probability [%]* |
|---|---|---|---|
| P1<br>4th order | 7.00<br>13.00 | -4.08 | -0.001 |
| S1<br>4th order | 12.50<br>12.50 | -0.26 | 0 |
| C5 | 5.42 | -1.23 | -0.001 |
| C6 | 6.21 | -2.58 | -0.002 |
| C9 | 11.28 | -4.97 | -0.003 |
| C10 | 11.33 | -8.13 | -0.008 |
| C11 | 15.8l8 | -27.05 | -0.029 |
| C12 | 9.94 | -5.06 | -0.004 |
| C16 | 11.70 | -1.06 | -0.002 |
| C17 | 10.11 | -14.63 | -0.02 |
| C18 | 8.91 | -3.54 | -0.002 |
| C20 | 24.36 | -72.97 | -0.152 |
| C21 | 6.89 | -6.24 | -0.005 |
| C22 | 9.59 | -2.73 | -0.004 |
| C23 | 10.22 | -2.05 | -0.002 |
| C24 | 23.95 | -19.47 | -0.028 |
| C25 | 18.33 | -40.21 | -0.091 |
| C26 | 13.66 | -16.25 | -0.03 |

### S2.5.2. Kuhs' Rule

For the refinement of SPAnPS, Gram-Charlier parameters in violation of Kuhs' rule (Kuhs, 1992) had to be introduced in order to successfully model the residual density around these heavier atoms. For all introduced Gram-Charlier coefficients, various quality indicators were examined (see Table S4) (Herbst-Irmer *et al.*, 2013). In the case of P1, the highest Gram-Charlier coefficients of 4$^{th}$ order refines to high significance of 13$\sigma$ and can therefore be expected to be reasonable. As reported by Herbst-Irmer *et al. (Herbst-Irmer et al., 2013)*, Kuhs' rule may be too strict for heavier atoms such as sulphur or phosphorous.

**Table S9** Maximum required resolution for refinement of meaningful Gram-Charlier coefficients (GCCs) according to Kuhs' rule taken from output files of *XDPDF* in the *XD2016* program suite (Volkov *et al.*, 2016). The relevant limits for the refined parameters are highlighted. The requirements are fulfilled for all atoms except P1. All resolutions given in $\sin(\theta/\lambda)$.

| | *Min. res. required for GCC of nth order (Kuhs' rule)* | | *Maximum order of refined GCCs (maximum resolution of experiment: 1.136)* |
|---|---|---|---|
| | n=3 | n=4 | |
| S1 | 0.81 | **0.94** | 4th |
| P1 | 1.06 | **1.22** | **4th** |
| C5 | **0.95** | 1.09 | 3rd |
| C6 | **0.94** | 1.08 | 3rd |
| C7 | **0.99** | 1.14 | 3rd |
| C9 | **0.88** | 1.01 | 3rd |
| C10 | **0.8** | 0.92 | 3rd |
| C11 | **0.82** | 0.95 | 3rd |
| C12 | **0.88** | 1.01 | 3rd |
| C16 | **0.78** | 0.9 | 3rd |
| C17 | **0.81** | 0.94 | 3rd |
| C18 | **0.89** | 1.02 | 3rd |
| C20 | **0.66** | 0.76 | 3rd |
| C21 | **0.78** | 0.9 | 3rd |
| C22 | **0.71** | 0.82 | 3rd |
| C23 | **0.63** | 0.73 | 3rd |

| | | | |
|---|---|---|---|
| C24 | **0.6** | 0.7 | 3rd |
| C25 | **0.6** | 0.69 | 3rd |
| C26 | **0.66** | 0.77 | 3rd |

**Table S10** Similarity indices calculated with *APD-Toolkit* (given in percent) for individual atoms of SPAnPS (Whitten & Spackman, 2006). Highlighted H-atoms are bonded to carbon atoms without refined anharmonic motion. Mean values excluding the C(sp3)-bonded H-Atoms H20A, H20B and H20C are denoted in brackets.

| | SHADE | APD | noquadru | quadru | HARt |
|---|---|---|---|---|---|
| **H4** | 1.277996 | 1.32334 | 0.156175 | 0.255681 | 2.340025 |
| H5 | 0.295186 | 0.432937 | 0.701225 | 0.159472 | 3.242928 |
| H6 | 0.39279 | 0.434172 | 2.245104 | 9.218902 | 2.153913 |
| **H7** | 1.793094 | 1.883624 | 4.475757 | 6.184401 | 1.462236 |
| H9 | 0.474916 | 0.502787 | 2.048449 | 3.686319 | 1.975668 |
| H10 | 0.603963 | 0.677014 | 3.284645 | 1.034371 | 2.208422 |
| H11 | 0.592998 | 0.667175 | 3.128941 | 1.93668 | 1.355325 |
| H12 | 0.875104 | 0.982627 | 1.124677 | 1.579796 | 1.299161 |
| **H13** | 0.747814 | 0.787244 | 1.332004 | 1.171786 | 1.354475 |
| **H15** | 0.821395 | 0.761641 | 3.919144 | 3.189214 | 1.224932 |
| H16 | 1.671122 | 1.786693 | 7.171311 | 17.363715 | 1.522358 |
| H17 | 0.234541 | 0.288759 | 1.375807 | 4.371084 | 1.196601 |
| **H18** | 0.324927 | 0.426291 | 2.375504 | 5.030602 | 0.813286 |
| H19 | 0.667183 | 0.76633 | 1.956254 | 1.628834 | 2.34336 |
| H20A* | 5.013252 | 5.480959 | 16.350949 | 18.00752 | 1.264353 |
| H20B* | 4.42349 | 4.372896 | 8.493924 | 13.090989 | 5.482734 |
| H20C* | 1.415201 | 1.495886 | 6.435485 | 6.31627 | 1.983661 |
| H22 | 0.910069 | 1.045332 | 0.198398 | 7.553271 | 1.620906 |
| H23 | 8.463898 | 8.676744 | 0.409556 | 8.640706 | 1.237257 |
| H24 | 1.471806 | 1.368654 | 0.051146 | 8.914029 | 2.340025 |

| | | | | | |
|---|---|---|---|---|---|
| H25 | 2.247687 | 2.282575 | 0.260131 | 13.878027 | 3.242928 |
| H26 | 0.687198 | 0.758794 | 0.096086 | 5.125898 | 2.153913 |
| $\langle S_{NX} \rangle$ | 5.311726 (6.288071) | 1.911069 (3.072303) | 1.360670 (1.691022) | 1.292299 (1.609347) | 1.899032 (3.446750) |
| $\langle S_{NX} \rangle$ No anharm | 2.4859832 | 2.3678668 | 1.1044358 | 1.0614964 | 1.7450056 |

**Table S11** Figures of Merit of SPAnPS with inclusion of the three H-atoms bonded with the sp3-hybridized C-atom of the guest toluene molecule.

| Method | ⟨DMSDA⟩ | $S_{NX}$ | $\langle U_X^{ii}/U_N^{ii} \rangle$ | $\langle \lvert \Delta U_{X-N}^{ii} \rvert \rangle$ | $\langle \lvert \Delta U_{X-N}^{ij} \rvert \rangle$ | wRMSD |
|---|---|---|---|---|---|---|
| Neutron | 96 | - | - | - | - | - |
| SHADE | 44 | 4.20 | 0.81(13) | 0.019(10) | 0.0093(7) | - |
| APD-Toolkit | 63 | 3.05 | 0.86(13) | 0.013(10) | 0.0071(7) | - |
| Aniso without H-Q0 | 154 | 1.68 | 0.94(7) | 0.000(4) | 0.000(3) | 13.69 |
| Aniso with H-Q0 | 158 | 1.60 | 0.96(7) | 0.004(4) | 0.002(3) | 16.24 |
| HARt* | 206 | 3.46 | 1.19(11) | 0.011(6) | 0.007(5) | 3.44 |

### S2.6. Fingerprint Plot of Intermolecular Close Contacts in SPAnPS

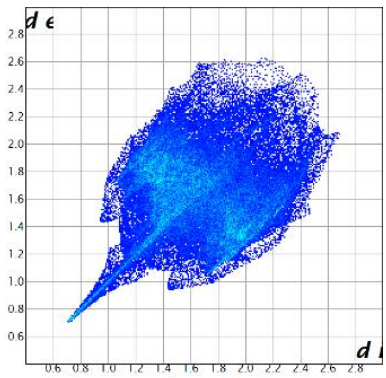


**Figure S13** Fingerprint plot of SPAnPS generated with *CrystalExplorer 17.5* (Turner *et al.*, 2018).

### S2.7. Calculated Intermolecular Interaction Energies

For "Neutron Data (tab. distances)", calculations were performed based on a refinement with ADPs from neutron results and C-H bond distances fixed to values provided by the *INVARIOM* database (1.08225 Å).

**Table S12** Top: Interaction energies between H12 / H13 and the toluene molecule located over the anthracene moiety. Bottom: Properties at the intermolecular BCP between H8 - C30 as well as interaction energies between H22 an the anthracene moiety. All energies given in kJ/mol.

| | H12 ···toluene | | | | H13 ···toluene | | | |
|---|---|---|---|---|---|---|---|---|
| | $E_{\mathrm{ES}}$ | $E_{\mathrm{ex-rep}}$ | $E_{\mathrm{disp}}$ | $E_{\mathrm{tot}}$ | $E_{\mathrm{ES}}$ | $E_{\mathrm{ex-rep}}$ | $E_{\mathrm{disp}}$ | $E_{\mathrm{tot}}$ |
| Neutron Data | -3.3 | 0.9 | -1.6 | -2.4 | -4.6 | 10.0 | -3.7 | 1.7 |
| Neutron Data (tab. distances) | -3.6 | 0.9 | -1.6 | -2.6 | -5.5 | 6.2 | -3.7 | 0.7 |
| SHADE | -2.0 | 2.5 | -1.6 | -1.1 | -2.9 | 9.8 | -3.7 | 3.2 |
| APD | -2.7 | 2.5 | -1.6 | -1.8 | -3.7 | 9.9 | -3.7 | 2.4 |
| Aniso-H | -3.5 | 2.5 | -1.6 | -2.6 | -5.5 | 9.8 | -3.7 | 0.6 |
| Aniso-H (no Q0) | -3.4 | 2.5 | -1.6 | -2.5 | -5.3 | 9.8 | -3.7 | 0.8 |

| | H22 ···anthracene | | | |
|---|---|---|---|---|
| | $E_{\mathrm{ES}}$ | $E_{\mathrm{ex-rep}}$ | $E_{\mathrm{disp}}$ | $E_{\mathrm{tot}}$ |
| Neutron Data | -7.2 | 11.3 | -4.8 | -0.8 |
| Neutron Data (tab. distances) | -7.0 | 11.3 | -4.8 | -0.5 |
| SHADE | -4.8 | 11.3 | -4.8 | 1.7 |
| APD | -5.4 | 11.2 | -4.8 | 0.9 |
| Aniso | -6.4 | 11.2 | -4.8 | 0.0 |
| Aniso-H (no Q0) | -6.1 | 11.2 | -4.8 | 0.4 |

### S2.8. List of Evaluated BCPs between the Toluene Molecule and the Anthracene Moiety

The observed electron densities at the investigated intermolecular BCPs are rather small. The standard uncertainties of the BCPs and Laplacian are of the same order of magnitude as the values their selves and should therefore be treated carefully regarding their validity.

**Table S13** Properties at the BCP between X4_H22 and X3_C3 of SPAnPS. X4_H22 is generated from the asymmetric unit by applying the symmetry operation 1/2 + X, 1/2 - Y, 1/2 + Z to the toluene molecule. X3_C3 is generated from the asymmetric unit by applying the symmetry operation – X+1, - Y+1, - Z+2 to the half of the SPAnPS-molecule present in it.

| | $\rho$ | $\nabla^2\rho(\boldsymbol{r})$ | $R_{ij}$ | *d1* | *d2* | *Hessian Eigenvalues* | | | $\varepsilon$ |
|---|---|---|---|---|---|---|---|---|---|
| *Neut* | 0.05 | 0.39 | 2.8679 | 1.1199 | 1.748 | -0.14 | -0.08 | 0.62 | 0.76 |
| *Neutron Data (tab. distances)* | 0.05 | 0.393 | 2.8679 | 1.1199 | 1.748 | -0.14 | -0.08 | 0.62 | 0.76 |
| *SHADE_H* | 0.04 | 0.44 | 2.8562 | 1.0911 | 1.7651 | -0.11 | -0.06 | 0.61 | 0.95 |
| *APD-H* | 0.05 | 0.43 | 2.8635 | 1.1038 | 1.7597 | -0.12 | -0.06 | 0.62 | 0.89 |
| *Aniso-H* | 0.05 | 0.41 | 2.8642 | 1.1148 | 1.7493 | -0.14 | -0.07 | 0.62 | 0.85 |
| *Aniso-H (no Q0)* | 0.05 | 0.42 | 2.863 | 1.1095 | 1.7535 | -0.13 | -0.07 | 0.62 | 0.88 |

**Table S14** Properties at the BCP between H12 and X4_C24 of SPAnPS. X4_C24 is generated from the asymmetric unit by applying the symmetry operation 1/2 + X, 1/2 - Y, 1/2 + Z to the toluene molecule.

| | $\rho$ | $\nabla^2\rho(\boldsymbol{r})$ | $R_{ij}$ | *d1* | *d2* | *Hessian Eigenvalues* | | | $\varepsilon$ |
|---|---|---|---|---|---|---|---|---|---|
| *Neutron Data* | 0.02 | 0.23 | 3.1793 | 1.2765 | 1.9028 | -0.05 | -0.03 | 0.31 | 1.04 |
| *Neutron Data (tab. distances)* | 0.02 | 0.23 | 3.1793 | 1.2765 | 1.9028 | -0.05 | -0.03 | 0.31 | 1.04 |
| *SHADE_H* | 0.02 | 0.26 | 3.2171 | 1.2914 | 1.9257 | -0.05 | -0.01 | 0.32 | 2.65 |
| *APD-H* | 0.02 | 0.26 | 3.242 | 1.2854 | 1.9566 | -0.05 | -0.01 | 0.33 | 2.91 |
| *Aniso-H* | 0.02 | 0.25 | 3.1861 | 1.2758 | 1.9103 | -0.05 | -0.02 | 0.32 | 1.32 |
| *Aniso-H (no Q0)* | 0.02 | 0.25 | 3.197 | 1.2763 | 1.9207 | -0.05 | -0.02 | 0.33 | 1.56 |

**Table S15** Properties at the BCP between H13 and X4_C22 of SPAnPS. X4_C22 is generated from the asymmetric unit by applying the symmetry operation 1/2 + X, 1/2 - Y, 1/2 + Z to the toluene molecule.

| | $\rho$ | $\nabla^2\rho(\boldsymbol{r})$ | $R_{ij}$ | *d1* | *d2* | *Hessian Eigenvalues* | | | $\varepsilon$ |
|---|---|---|---|---|---|---|---|---|---|
| *Neutron Data* | 0.05 | 0.43 | 2.805 | 1.1052 | 1.6998 | -0.15 | -0.07 | 0.65 | 1.13 |
| *Neutron Data (tab. distances)* | 0.05 | 0.43 | 2.805 | 1.1052 | 1.6998 | -0.15 | -0.07 | 0.65 | 1.13 |
| *SHADE_H* | 0.05 | 0.51 | 2.8429 | 1.1016 | 1.7414 | -0.11 | -0.02 | 0.64 | 4.01 |
| *APD-H* | 0.05 | 0.48 | 2.8312 | 1.0902 | 1.741 | -0.14 | -0.05 | 0.67 | 1.52 |
| *Aniso-H* | 0.05 | 0.46 | 2.8186 | 1.1117 | 1.7069 | -0.14 | -0.05 | 0.66 | 1.6 |
| *Aniso-H (no Q0)* | 0.05 | 0.48 | 2.8275 | 1.1075 | 1.72 | -0.14 | -0.05 | 0.66 | 1.8 |

### S3. Additional Information for SPAnH

Further details about this structure can be found in the publication by Herbst-Irmer *et al.* (Herbst-Irmer *et al.*, 2013) mentioned in the main article. Only specific differences to the approach of the authors will be mentioned here in detail.

#### S3.1. Refinement Strategy

**Table S16** Final refinement strategy for SPAnH with isotropic hydrogen atoms. Starting values for multipole and $\kappa$- parameters were obtained from the *INVARIOM* database (Dittrich *et al.*, 2013) using the software *InvariomTool*. The scale factor is refined in every step. Red denotes newly added parameters. Green denotes the final refinement step with fixed C-H bond distances At the beginning of the refinement, only reflections with a significance of at least $3\sigma$ are taken into account ("sigobs 3"). This limitation is released in step 8. A test for overfitting was performed using a $R_{\mathrm{cross}}$ as validation tool.(Krause *et al.*, 2017b). Abbreviations: M: monopoles; D: dipoles; Q: quadrupoles; O: octupoles; H: hexadecapoles, U: Uij, k: kappa, U3/4 (atom name): Gram Charlier 3$^{\mathrm{rd}}$/4$^{\mathrm{th}}$ order, nosym: no local symmetry constraints, nocon: no chemical constraints, *d/p*: data to parameter ratio, $d_1/p_{\mathrm{m}}$: ratio of low resolution data ( up to 1 Å) to multipole parameter.

| Step | Parameters | #param | #data | $d/p$ | $d_1/p_m$ | $\sigma$ cut-off | $R(F^2)$ |
|---|---|---|---|---|---|---|---|
| 1 | SCALE | 1 | 37280 | 37280 | None | 3 | 0.0267 |
| 2 | U | 505 | 37280 | 73.82 | None | 3 | 0.0236 |
| 3 | MDQOHUxyz$\kappa$ | 641 | 37280 | 58.16 | 50.96 | 3 | 0.0202 |
| 4 | xyz(H) | 115 | 4025 | 35 | None | 3 | 0.0191 |
| 5 | MDQOHUxyz$\kappa$ | 641 | 37280 | 58.16 | 50.96 | 3 | 0.0191 |
| 6 | $\kappa'$ | 12 | 37280 | 3106.67 | None | 3 | 0.0189 |
| 7 | MDQOHUxyz$\kappa$ | 641 | 37280 | 58.16 | 50.96 | 3 | 0.0189 |
| 8 | Sigobs 0 | 641 | 41640 | 64.96 | 52.16 | 0 | 0.0189 |
| 9 | MDQOHUxyz$\kappa$ U3 (S2, P2) | 721 | 41640 | 57.75 | 52.16 | 0 | 0.0166 |
| 10 | MDQOHUxyz$\kappa$ U3, U4 (S2) | 736 | 41640 | 56.58 | 52.16 | 0 | 0.0165 |
| 11 | MDQOHUxyz$\kappa$ U3 (C5), U4 | 746 | 41640 | 55.82 | 52.16 | 0 | 0.0164 |
| 12 | MDQOHUxyz$\kappa$ U3 (C43-46), U4 | 786 | 41640 | 52.98 | 52.16 | 0 | 0.0163 |
| 13 | MDQOHUxyz$\kappa$ U3 (C24), U4 | 796 | 41640 | 52.31 | 52.16 | 0 | 0.0162 |
| 14 | U3 (C12), U4 | 806 | 41640 | 51.66 | 52.16 | 0 | 0.0162 |
| 15 | $U_{ij}$, XYZ, M, D, Q, O, H, $\kappa$, U3 (S2), U4 | 816 | 41640 | 51.03 | 52.16 | 0 | 0.0161 |
| 16 | Uij unconstrained | 1044 | 41640 | 39.89 | 52.16 | 0 | 0.0149 |
| 17 | H(xyz) without RESET | 1158 | 41640 | 35.96 | 52.16 | 0 | 0.0149 |

### S3.2. Release of Constraints

| Step | Parameters | #param | #data | $d/p$ | $d_1/p_m$ | $\sigma$ cut-off | Res. [Å-1] | $R(F^2)$ |
|---|---|---|---|---|---|---|---|---|
| 1-17 | As before | | | | | | | |
| 18 | Nocon Anthracene | 1476 | 41640 | 28.21 | 17.84 | 0 | 1.10 | 0.0146 |
| 19 | Nosymm P | 1476 | 41640 | 28.21 | 17.84 | 0 | 1.10 | 0.0146 |
| 20 | Nosymm S | 1514 | 41640 | 27.5 | 16.48 | 0 | 1.10 | 0.0145 |
| 21 | Nosymm | 1882 | 41640 | 22.13 | 9.1 | 0 | 1.10 | 0.0141 |
| 22 | Nocon | 3382 | 41640 | 12.31 | 3.45 | 0 | 1.10 | 0.0131 |

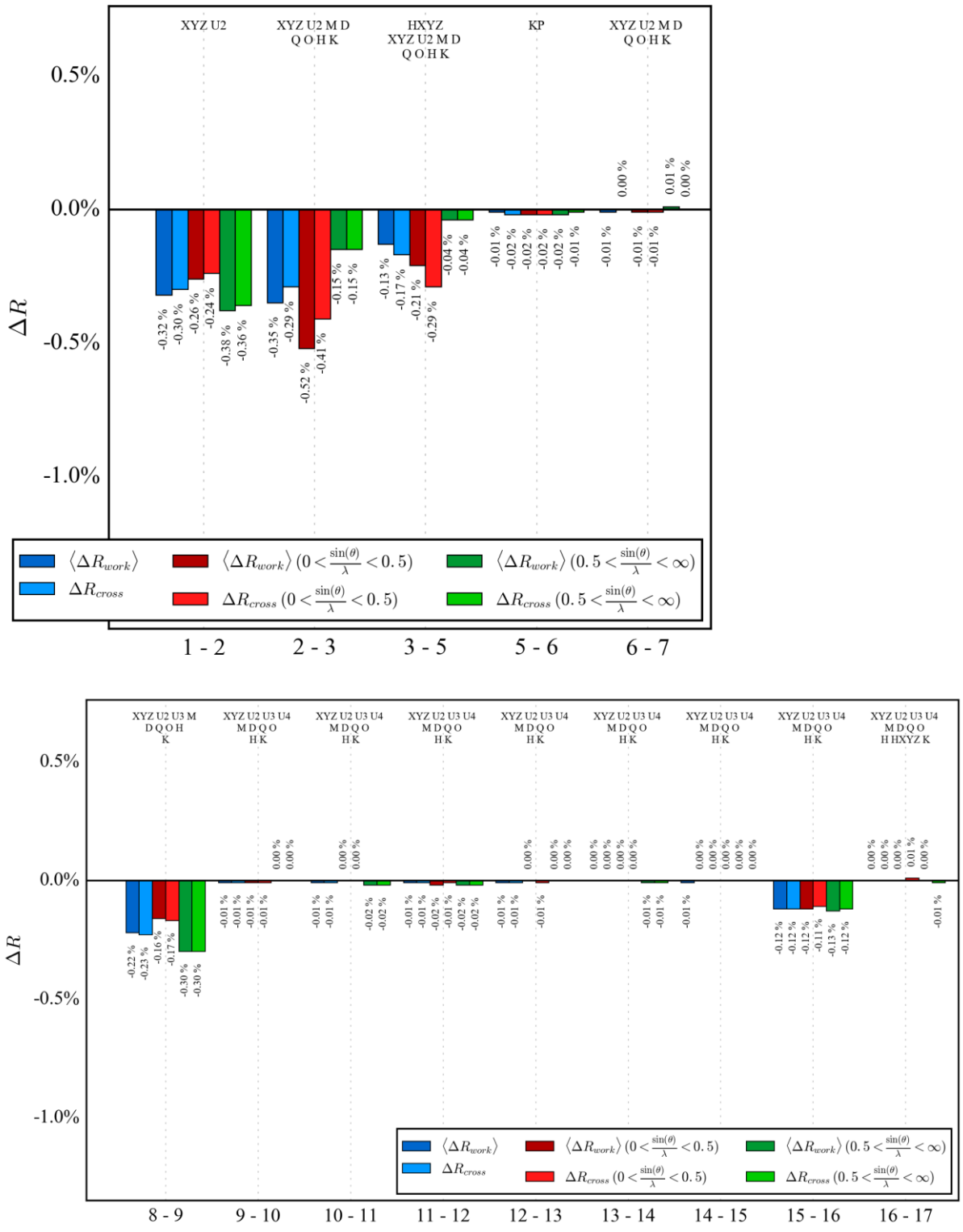


**Figure S14** Cross-validation output plot for steps included in the final refinement of SPAnH. The generally joined improvement of both $R_{work}$ and $R_{cross}$ indicates that all introduced parameters are meaningful.

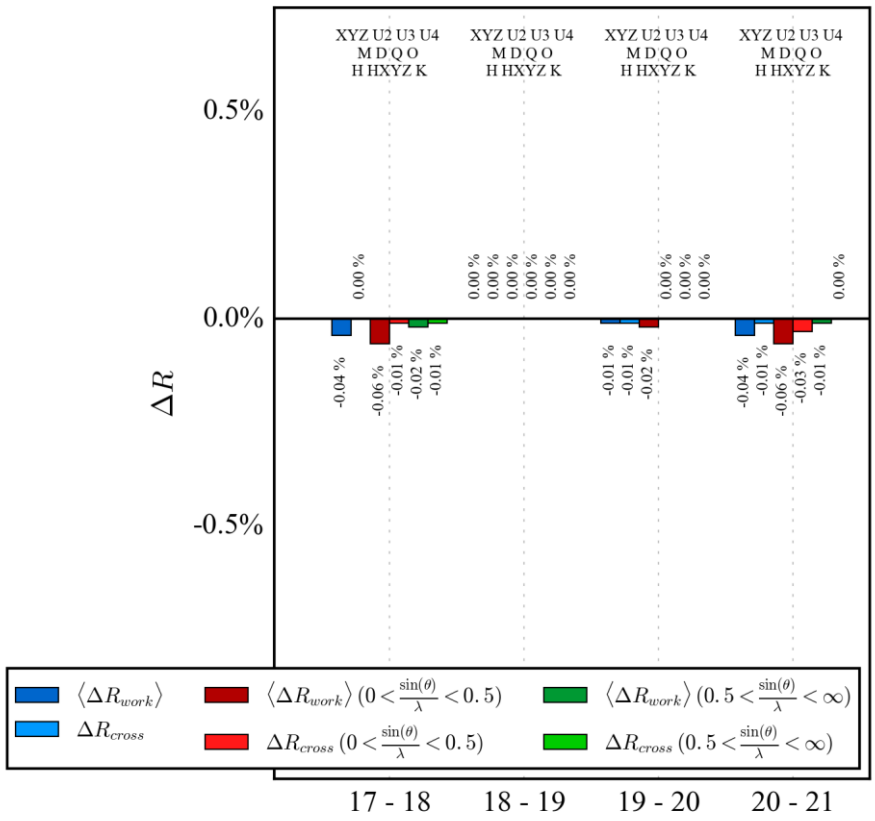


**Figure S15** Cross-validation output plot for steps excluded from the final refinement of SPAnH. All steps include a worsening of the $R_{cross}$ while $R_{work}$ stays constant or improves. This is a sign of overfitting.

### S3.3. Residuals after Final Step with Anisotropic H and Fixed C-H Distances

**Neutron ADPs with Neutron Distances**

| | | | | | | | | |
|---|---|---|---|---|---|---|---|---|
| $R(F)$ | = | 0.0139 | $R_{all}(F)$ | = | 0.0155 | $R_w(F)$ | = | 0.0113 |
| $R(F^2)$ | = | 0.0148 | $R_{all}(F^2)$ | = | 0.0152 | $R_w(F^2)$ | = | 0.0217 |
| GOF*w* | = | 1.5616 | GOF | = | 1.5616 | $N_{ref}/N_v$ | = | 51.0294 |

**SHADE**

| | | | | | | | | |
|---|---|---|---|---|---|---|---|---|
| $R(F)$ | = | 0.0141 | $R_{all}(F)$ | = | 0.0157 | $R_w(F)$ | = | 0.0115 |
| $R(F^2)$ | = | 0.0151 | $R_{all}(F^2)$ | = | 0.0155 | $R_w(F^2)$ | = | 0.0222 |
| GOF*w* | = | 1.5918 | GOF | = | 1.5918 | $N_{ref}/N_v$ | = | 51.0294 |

**APD-Toolkit**

| | | | | | | | | |
|---|---|---|---|---|---|---|---|---|
| $R(F)$ | = | 0.0140 | $R_{all}(F)$ | = | 0.0156 | $R_w(F)$ | = | 0.0114 |
| $R(F^2)$ | = | 0.0149 | $R_{all}(F^2)$ | = | 0.0153 | $R_w(F^2)$ | = | 0.0218 |
| GOF*w* | = | 1.5673 | GOF | = | 1.5673 | $N_{ref}/N_v$ | = | 51.0294 |

**Aniso without H-Q0**

| | | | | | | | | |
|---|---|---|---|---|---|---|---|---|
| $R(F)$ | = | 0.0140 | $R_{all}(F)$ | = | 0.0156 | $R_w(F)$ | = | 0.0114 |
| $R(F^2)$ | = | 0.0151 | $R_{all}(F^2)$ | = | 0.0155 | $R_w(F^2)$ | = | 0.0219 |
| GOF*w* | = | 1.5747 | GOF | = | 1.5747 | $N_{ref}/N_v$ | = | 39.9233 |

**Aniso with H-Q0**

| | | | | | | | | |
|---|---|---|---|---|---|---|---|---|
| $R(F)$ | = | 0.0138 | $R_{all}(F)$ | = | 0.0154 | $R_w(F)$ | = | 0.0112 |
| $R(F^2)$ | = | 0.0145 | $R_{all}(F^2)$ | = | 0.0149 | $R_w(F^2)$ | = | 0.0214 |
| GOF*w* | = | 1.5408 | GOF | = | 1.5408 | $N_{ref}/N_v$ | = | 39.8851 |

**Table S17** Similarity indices (Whitten & Spackman, 2006) calculated with *APD-Toolkit* (given in percent) for individual atoms of SPAnH. Highlighted H-atoms are bonded to carbon atoms without refined anharmonic motion.

| | SHADE | APD | noquadru | quadru | HARt |
|---|---|---|---|---|---|
| **H3** | 0.735439 | 0.250514 | 7.354701 | 1.641876 | 4.07361 |
| **H4** | 0.38486 | 0.250697 | 4.283626 | 1.04242 | 3.111311 |
| **H5** | 1.59031 | 0.811745 | 2.659268 | 0.335058 | 0.92858 |
| **H6** | 0.797685 | 0.48231 | 2.690543 | 0.234528 | 0.83028 |
| **H8** | 0.094343 | 0.180266 | 7.975837 | 4.333563 | 5.077343 |
| **H10** | 0.431375 | 0.13544 | 5.783256 | 2.003877 | 2.484346 |
| **H11** | 0.547429 | 0.071501 | 2.560531 | 0.291067 | 1.463826 |
| H12 | 1.943098 | 1.083164 | 1.999171 | 0.094068 | 0.814161 |
| **H13** | 2.728587 | 1.931264 | 2.730781 | 0.637403 | 0.603542 |
| **H16** | 1.18959 | 1.687781 | 2.981933 | 0.450013 | 0.666627 |
| **H17** | 0.699078 | 0.610918 | 2.783831 | 0.378383 | 1.658324 |
| **H18** | 1.111575 | 0.703224 | 2.839813 | 0.299353 | 1.148406 |
| **H19** | 0.810532 | 0.564725 | 2.766635 | 0.352779 | 0.880654 |
| **H(20)** | 0.887128 | 0.252982 | 2.583762 | 0.405157 | 0.624032 |
| **H22** | 1.03361 | 0.825128 | 2.695552 | 0.541161 | 1.862767 |
| **H23** | 1.501707 | 0.638279 | 3.499417 | 0.622953 | 1.072131 |
| H24 | 1.592182 | 0.586143 | 2.958628 | 0.533845 | 1.214036 |
| **H25** | 1.001255 | 0.505003 | 1.376693 | 0.134755 | 0.285275 |
| **H26** | 1.017398 | 1.204453 | 4.427437 | 0.718329 | 2.582598 |
| **H(29)** | 0.403484 | 0.069079 | 3.984139 | 0.689565 | 1.212212 |
| **H30** | 0.284538 | 0.337816 | 2.784749 | 0.321147 | 2.202443 |
| **H31** | 0.78288 | 0.247521 | 2.691152 | 0.342819 | 0.663706 |
| **H32** | 0.726718 | 0.439748 | 2.135865 | 0.628039 | 0.612454 |
| **H34** | 0.173897 | 0.06761 | 3.626514 | 0.849848 | 1.593553 |
| **H36** | 1.292339 | 0.78188 | 2.247399 | 0.581743 | 1.53922 |
| **H37** | 1.478092 | 0.446 | 2.170788 | 0.129029 | 0.719739 |

| | | | | | |
|---|---|---|---|---|---|
| **H38** | 1.818987 | 0.102386 | 2.094934 | 0.098027 | 0.777769 |
| **H39** | 1.60285 | 0.619808 | 5.668066 | 1.58488 | 2.169242 |
| **H42** | 0.998851 | 1.109014 | 3.549686 | 0.788704 | 2.323013 |
| H43 | 7.414878 | 7.209315 | 3.368994 | 4.65283 | 5.758804 |
| H44 | 2.285165 | 0.340706 | 1.42859 | 0.182815 | 0.771767 |
| H45 | 5.310498 | 6.88449 | 3.093478 | 5.907403 | 4.594388 |
| H46 | 2.1169 | 0.831891 | 1.270228 | 0.83551 | 0.772535 |
| H48 | 3.642694 | 0.541393 | 1.999425 | 0.510603 | 0.943654 |
| H49 | 6.064898 | 1.635144 | 0.930977 | 0.201076 | 1.065336 |
| H50 | 6.189183 | 0.767809 | 1.674536 | 0.327044 | 1.299554 |
| H51 | 4.339047 | 0.79767 | 1.96537 | 0.380577 | 1.186696 |
| H52 | 0.990255 | 1.014624 | 3.821436 | 0.698866 | 1.821718 |
| $\langle S_{NX} \rangle$ | 1.78982461 | 0.97419582 | 3.09099318 | 0.91476613 | 1.66867505 |
| $\langle S_{NX} \rangle$ No anharm. | 0.96757544 | 0.56767007 | 3.44247807 | 0.75690652 | 1.59877789 |

### S3.4. Fingerprint Plot of Intermolecular Close Contacts in SPAnH

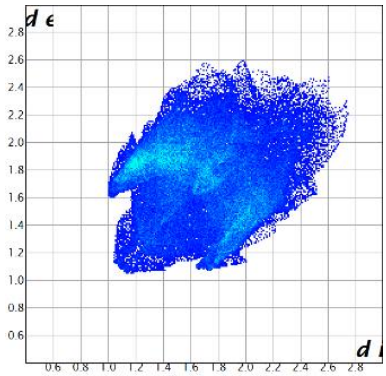


**Figure S16** Fingerprint plot of the first molecule in the asymmetric unit of SPAnH generated with *CrystalExplorer 17.5* (Turner *et al.*, 2018).

### S3.5. Calculated Intermolecular Interaction Energies

For "Neutron Data (tab. distances)", calculations were performed based on a refined with ADPs from Neutron results and C-H bond distances fixed to values provided by the *INVARIOM* database (1.08225 Å).

**Table S18** Interaction energies between H8 / H10 and the neighbouring anthracene moiety. The given distances are calculated between the H-Atom and the centre of the anthracene moiety. All energies given in kJ/mol.

| | $E_{\mathrm{ES}}$ | $E_{\mathrm{ex-rep}}$ | $E_{\mathrm{disp}}$ | $E_{\mathrm{tot}}$ | $E_{\mathrm{ES}}$ | $E_{\mathrm{ex-rep}}$ | $E_{\mathrm{disp}}$ | $E_{\mathrm{tot}}$ |
|---|---|---|---|---|---|---|---|---|
| Neutron Data | -9.3 | 15.5 | -5.6 | 0.5 | -11.4 | 25.9 | -8.4 | 6.1 |
| Neutron Data (tab. distances) | -9.3 | 15.5 | -5.6 | 0.5 | -11.4 | 25.9 | -8.4 | 6.1 |
| SHADE | -8.2 | 15.1 | -5.5 | 1.4 | -10.3 | 25.9 | -8.5 | 7.2 |
| APD | -8.6 | 15.1 | 9.6 | 0.9 | -10.7 | 25.9 | -8.5 | 6.7 |
| Aniso-H | -8.8 | 15.1 | -5.5 | 0.7 | -11.0 | 25.9 | -8.5 | 6.4 |
| Aniso-H (no Q0) | -5.3 | 15.1 | -5.5 | 4.3 | -6.1 | 25.9 | -8.5 | 11.4 |

### S3.6. List of Evaluated BCP between Neighbouring SPAnH Molecules

The observed electron densities at the investigated intermolecular BCPs are rather small. The standard uncertainties of the BCPs and Laplacian are of the same order of magnitude as the values theirselves and should therefore be treated careful regarding their validity.

**Table S19** Properties of the BCP between H8 and X2_C30. X2_C30 is generated from the asymmetric unit by applying the symmetry operation –X, 1-Y, 2-Z to the SPAnH molecule.

| | $\rho$ | $\nabla^2\rho(\boldsymbol{r})$ | $R_{ij}$ | *d1* | *d2* | *Hessian Eigenvalues* | | | $\varepsilon$ |
|---|---|---|---|---|---|---|---|---|---|
| *Neutron Data* | 0.05 | 0.45 | 2.7512 | 1.0816 | 1.6696 | -0.16 | -0.09 | 0.71 | 0.8 |
| *Neutron Data (tab. distances)* | 0.05 | 0.45 | 2.7512 | 1.0816 | 1.6696 | -0.16 | -0.09 | 0.71 | 0.8 |
| *SHADE_H* | 0.05 | 0.49 | 2.7535 | 1.0752 | 1.6783 | -0.14 | -0.08 | 0.7 | 0.87 |
| *APD-H* | 0.05 | 0.467 | 2.7575 | 1.0838 | 1.6737 | -0.15 | -0.08 | 0.7 | 0.83 |
| *Aniso-H* | 0.05 | 0.46 | 2.7565 | 1.0801 | 1.6763 | -0.15 | -0.08 | 0.69 | 0.84 |
| *Aniso-H (no Q0)* | 0.03 | 0.51 | 2.8938 | 1.0918 | 1.802 | -0.07 | -0.02 | 0.6 | 2.13 |

**Table S20** Properties of the BCP between H10 and X2_C28. X2_C28 is generated from the asymmetric unit by applying the symmetry operation –X, 1-Y, 2-Z to the SPAnH molecule. The BCP given for Aniso-H (no Q0) was found between H10 and X2_C27 instead. The BCP given for Aniso-H (no Q0) was found between H10 and X2_C40 instead. Both of these atoms are generated from the aforementioned symmetry operation.

| | $\rho$ | $\nabla^2\rho(\boldsymbol{r})$ | $R_{ij}$ | *d1* | *d2* | *Hessian Eigenvalues* | | | $\varepsilon$ |
|---|---|---|---|---|---|---|---|---|---|
| *Neutron Data* | 0.07 | 0.59 | 2.7146 | 1.0316 | 1.683 | -0.2 | -0.08 | 0.86 | 1.57 |
| *Neutron Data (tab. distances)* | 0.07 | 0.585 | 2.7146 | 1.0316 | 1.683 | -0.2 | -0.08 | 0.86 | 1.57 |
| *SHADE_H* | 0.06 | 0.63 | 2.7122 | 1.0232 | 1.689 | -0.17 | -0.06 | 0.86 | 2.1 |
| *APD-H* | 0.07 | 0.61 | 2.7148 | 1.0286 | 1.6862 | -0.19 | -0.07 | 0.86 | 1.75 |
| *Aniso-H* | 0.07 | 0.60 | 2.7067 | 1.0247 | 1.682 | -0.19 | -0.07 | 0.85 | 1.71 |
| *Aniso-H (no Q0)* | 0.051 | 0.633 | 2.7452 | 1.1086 | 1.6365 | -0.1 | -0.05 | 0.79 | 0.91 |